



Deactivating species in the transformation of crude bio-oil with methanol into hydrocarbons on a HZSM-5 catalyst

Beatriz Valle*, Pedro Castaño, Martin Olazar, Javier Bilbao, Ana G. Gayubo

Chemical Engineering Department, University of the Basque Country, P.O. Box 644, 48080 Bilbao, Spain

ARTICLE INFO

Article history:

Received 7 June 2011

Revised 8 September 2011

Accepted 9 October 2011

Available online 12 November 2011

Keywords:

Biorefinery

Bio-oil

Methanol

Coke

Deactivation

HZSM-5 zeolite

MTO process

ABSTRACT

A study has been carried out by using different techniques (TPO, FTIR, Raman, ^{13}C NMR, GC/MS of the coke dissolved in CH_2Cl_2) on the nature of the coke deposited on a HZSM-5 catalyst modified with Ni in the transformation of the crude bio-oil obtained by flash pyrolysis of lignocellulosic biomass (pine sawdust) into hydrocarbons. The reaction system has two steps in-line. In the first one, the components of crude bio-oil derived from the pyrolysis of biomass lignin are polymerized at $400\text{ }^\circ\text{C}$. In the second one, the remaining volatile oxygenates are transformed into hydrocarbons in a fluidized bed catalytic reactor at $450\text{ }^\circ\text{C}$. The reaction has been carried out with different bio-oil/methanol mass ratios in the feed (from 100/0 to 0/100). Co-feeding methanol significantly attenuates coke deposition, and the nature of the coke components varies according to the bio-oil/methanol ratio in the feed. When bio-oil is co-fed, the coke deposited on the catalyst has a significant content of oxygenates and oxo-aromatics and consists of two fractions, identified by temperature programmed oxidation, corresponding to external and internal coke in the zeolite crystals. The fraction of external coke is soluble in CH_2Cl_2 , with a high content of oxygenates and oxo-aromatics, and is generated by polymerization of products derived from biomass lignin pyrolysis activated by the zeolite acid sites. The fraction of coke retained within the zeolite crystals is partially insoluble and is formed by several routes: from the intermediates in the transformation of both methanol and bio-oil oxygenates into hydrocarbons; by evolution of the other coke fraction; from the hydrocarbons (with high aromatics content) in the reaction medium.

© 2011 Elsevier Inc. All rights reserved.

1. Introduction

Lignocellulosic biomass and its derivatives are an alternative feedstock for partially replacing petroleum as raw material for obtaining fuels, hydrocarbons for petrochemical synthesis and hydrogen [1–3]. The valorization of lignocellulosic biomass instead of coal and natural gas has the advantages of its renewable nature, i.e. no CO_2 net production, lower SO_2 and NO_x emissions and a worldwide availability.

The flash pyrolysis of lignocellulosic biomass provides a yield of around 70 wt.% of liquid (bio-oil), using simple technologies with small capital assets [4,5]. The bio-oil can be obtained in delocalized rural areas and subsequently stored and transported to a refinery (biorefinery) for its large-scale valorization.

Crude bio-oil is a polar and hydrophilic brown liquid, with a water content of around 30 wt.% (that obtained from herbaceous biomass may exceed 50 wt.%) and an oxygen content of 45–50 wt.%, as a result of water content and its oxygenated composition, with compounds (acids, alcohols, aldehydes, esters, ketones, phenols, guaiacols, syringols, sugars, furans and others) derived

from the fragmentation of biomass cellulose, hemicellulose and lignin [4,6,7]. Its heating value ($15\text{--}18\text{ MJ kg}^{-1}$), although limited by the water content, is interesting for its use as fuel [8]. However, the transformation of oxygenated compounds in the bio-oil by catalytic processes into hydrocarbons or H_2 is of greater interest [9].

The hydrocarbons can be obtained by cracking deoxygenation of flash pyrolysis primary products using an acid catalyst in situ in the pyrolysis reactor, by the catalytic fast pyrolysis (CFP) process [10–15] or with a catalytic bed in-line for processing the volatile compounds that leave the pyrolysis reactor [16–18].

From the perspective of sustainability and the development of a large-scale biorefinery concept, great attention has been paid to the co-feeding of bio-oil (and also other biomass derivatives such as glycerol) into refinery units, particularly FCC (fluidized catalytic cracking) units [19,20]. In order to gain knowledge on the effect of co-feeding bio-oil on product yield and quality, studies have been carried out on the catalytic cracking of model oxygenates in the bio-oil (such as phenol and guaiacol) with diesel under conditions similar to those in the FCC [21,22].

Gayubo et al. [23,24] have studied the transformation of bio-oil oxygenated compounds into hydrocarbons over HZSM-5 zeolite catalysts, proving that these reactions are very similar to the transformation of methanol/dimethyl ether into hydrocarbons over this

* Corresponding author.

E-mail address: beatriz.valle@ehu.es (B. Valle).

Nomenclature

C_{ci} , C_{cT}	content of i coke fraction in the catalyst ($i = 1$, thermal coke; $i = 2$, catalytic coke) and total coke content	$(m_{\text{oxygenates}})_{\text{inlet}}$	mass flow of oxygenates (MeOH, bio-oil) at the fluidized reactor inlet (g h^{-1})
E_i	activation energy for the combustion of i coke fraction (kJ mol^{-1})	P_{O_2}	partial pressure of oxygen in the gas for burning the coke, atm
k_i , k_i^*	kinetic constant for the combustion of i coke fraction at T temperature and at 550°C ($\text{atm}^{-1} \text{s}^{-1}$ and s^{-1})	R	constant of gases, $\text{kJ mol}^{-1} \text{K}^{-1}$
$(m_{\text{bio-oil}})_{\text{inlet}}$	mass flow of bio-oil oxygenated components at the fluidized reactor inlet (g h^{-1})	S_g	BET-specific surface ($\text{m}^2 \text{g}^{-1}$)
$(m_{\text{bio-oil}})_{\text{outlet}}$	mass flow of bio-oil oxygenated components at the fluidized reactor outlet (g h^{-1})	T	temperature (K)
$(m_i)_{\text{outlet}}$	mass flow of product lump i at the fluidized reactor outlet (g h^{-1})	$X_{\text{bio-oil}}$	bio-oil conversion
		X_i	lump i concentration, given as a mass fraction on a water-free basis
		Y_i	yield of product lump i

type of catalysts [25–27]. These similarities lie in: (i) the kinetic schemes for the formation of light olefins, paraffins and aromatics; (ii) the effect of lump concentrations in the reaction medium on the deactivation by catalytic coke deposition. In the formation of coke from furan (model compound of biomass) on a HZSM-5 zeolite catalyst, Chen and Huber [28] consider a hydrocarbon pool mechanism similar to that for methanol transformation, but with a different composition. These analogies open an interesting perspective for co-feeding bio-oil in the MTO process over HZSM-5 zeolite catalysts. Mentzel and Holm [29] have studied the co-feeding of bio-oil model compounds with methanol, ascertaining methanol effect on attenuating the deactivation by coke.

Nevertheless, the feasibility of using crude bio-oil in the aforementioned catalytic processes (particularly, the catalytic cracking in FCC and the MTO process) is curtailed by the problem associated with the polymerization of bio-oil oxygenated components above 80°C . The formation of a large amount of carbonaceous material (with a yield above 30 wt.%) hinders feeding crude bio-oil into the reactor, and furthermore, the catalyst undergoes rapid deactivation, and the flow inside the reactor is blocked [30]. Gayubo et al. [31] have ascertain the particular role of certain components (aldehydes, oxypheols, furfural and their derivatives) in the deposition of carbonaceous material and HZSM-5 zeolite catalyst deactivation in the transformation of a light bio-oil fraction.

Amongst the solutions studied in the literature for crude bio-oil valorization by catalytic transformation into hydrocarbons, the following are worth mentioning: (i) fractionation and valorization of a bio-oil fraction without polymerization problems, usually the aqueous fraction (with less content of lignin derivatives) or a fraction with low boiling point [32,33]; (ii) thermal degradation (accelerated ageing) to promote the separation of a polymerizable fraction [30,34,35]; (iii) hydrodeoxygenation to increase the H/C ratio and attenuate the subsequent deposition of carbonaceous material [36–38]; (iv) methanol co-feeding to increase the H/C ratio of the mixture [30]. The co-feeding of methanol with bio-oil is mandatory if methanol is used to stabilize the crude bio-oil during storage, for which at least 10 wt.% of methanol is required [39,40].

Other actions to improve the crude bio-oil, such as the esterification of bio-oil acids, either in-line in the output stream of the pyrolysis reactor [41] or by treating the collected bio-oil [42], are effective to reduce bio-oil acidity and corrosiveness, improving its viability as a fuel. However, they are not likely effective to reduce significantly the problem of lignin derivative polymerization.

Gayubo et al. [43] have proposed a two-step process (thermal and catalytic) in-line for the valorization of crude bio-oil (Fig. 1). The first step is to exhaust the polymerization, so that the remaining stream of treated bio-oil is transformed in the second step

(fluidized catalytic reactor) with few problems of thermal coke deposition over the catalyst. With this strategy, and co-feeding methanol with bio-oil, a high yield of light olefins [44] or aromatics [45] is obtained, using HZSM-5 selective catalysts that undergo limited deactivation by coke deposition and are liable to be regenerated [46]. The polymerization of certain bio-oil oxygenates in the first step at 400°C allows obtaining a solid (which is called pyrolytic lignin) with a composition and properties similar to those of the lignin derived from the production of paper pulp [43], which increases its valorization perspectives. The material balance for the two-step process and the significance of methanol content in the feed (Bio-oil/methanol) on this balance has been described in previous papers [30,43]. Two alternatives for the valorization of the pyrolytic lignin have been considered in Fig. 1: (i) gasification, in order to obtain methanol for stabilizing the bio-oil to be co-fed into the process, (ii) conventional pyrolysis, whose solid product (char) can be used as fuel, owing to its high heating value or can be subject to activation processes to obtain activated carbon for purification processes and for use as a support for metallic catalysts [47,48] or as acid catalyst [49].

A study has been conducted in this paper on the nature of the coke deposited on a HZSM-5 zeolite catalyst modified with Ni, which has been used in the two-step process shown in Fig. 1 with different crude bio-oil/methanol ratios in the feed. The objective is to identify the coke fractions of thermal and catalytic origin and their location within the catalyst. Another objective is to step further on the origin of the catalytic coke and its relationship with the reaction scheme by determining the role of methanol and bio-oil transformation steps in coke formation and the possible synergy between both reactants for coke formation.

2. Experimental

2.1. Bio-oil production and composition

The bio-oil has been obtained by flash pyrolysis at 450°C using a N_2 stream, in a plant pilot provided with a conical spouted bed reactor [4,10,11]. The feedstock was pine (*Pinus insignis*) sawdust with a particle size between 0.8 mm and 2 mm. The crude bio-oil used in this study corresponds to 80 wt.% of the entire bio-oil. Thus, in order to attain product reproducibility, the bio-oil studied is that collected in the condenser and in the ice-water trap, whereas that retained in the coalescence filter has been discarded. The composition of the crude bio-oil (Table 1) has been determined by GC/MS analyzer (Shimadzu QP2010S device) provided with a TBR-IMS column.) Product identification has been accomplished using the NIST 140 library. The detailed composition of individual

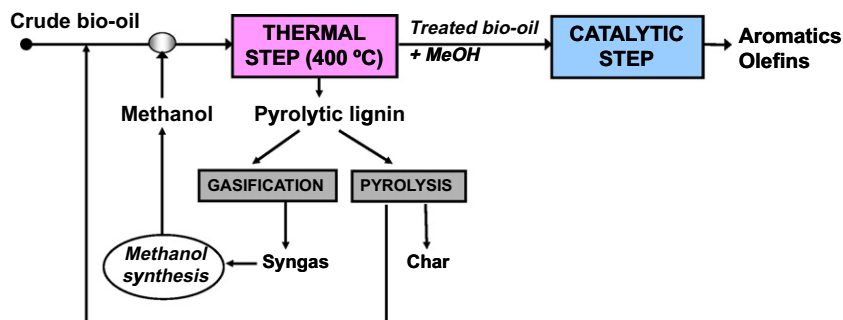


Fig. 1. Two-step process for the transformation of crude bio-oil into hydrocarbons.

Table 1

Component families of the crude bio-oil.

Components	wt.%
Acetic acid	15.3
Acetone	5.3
Other ketones	21.8
Other acids and esters	10.8
Hydroxyacetaldehyde	10.6
Other aldehydes	8.7
Phenols	8.2
Alcohols	11.6
Ethers	0.9
Levoglucosan	3.9
Others	1.3
Non-identified	1.6

components is shown in a previous paper [43]. The elemental composition is $\text{CH}_{1.84}\text{O}_{0.59}$, and the average molecular weight is 100.2 g mol^{-1} . The water content (48 wt.%) has been measured by gas chromatography (Agilent Micro GC 3000).

2.2. Catalyst

The catalyst has been prepared from commercial HZSM-5 zeolite (supplied by Zeolyst International) with $\text{SiO}_2/\text{Al}_2\text{O}_3 = 30$, which has been modified by incorporating 1 wt.% of Ni. This Ni content is suitable to achieve hydrothermal stability (important in a reaction medium with high content of steam), which gives the catalyst ability to recover its kinetic behaviour when it is used in reaction-regeneration cycles [50]. The commercial zeolite is supplied in ammonium form, and in order to obtain the acid form, it is calcined following a temperature ramp (up to 570°C). Impregnation with Ni was carried out by slowly adding a $\text{Ni}(\text{NO}_3)_2$ solution to the acid zeolite under vacuum (in a Rotavapor) at 80°C .

The modified zeolite was dried for 24 h at 110°C and subsequently agglomerated (by wet extrusion) with bentonite (Exaloid) and using alumina (Prolabo) calcined at 1000°C as inert charge. The proportion of each component in the catalyst is 25 wt.% zeolite, 45 wt.% bentonite and 30 wt.% alumina. The extrudates were dried at room temperature for 24 h. The particles were subsequently ground and sieved to a size between 0.15 and 0.25 mm, dried at 110°C for 24 h and calcined at 575°C for 2 h. This temperature is reached following a heating rate of 5°C min^{-1} and is suitable for dehydroxylation of strong acid sites so that the catalyst is hydrothermally stable [51]. The agglomeration provides the catalyst with the mechanical strength required to minimize the material loss by attrition in fluidized bed reactor. Moreover, zeolite crystals are embedded in a matrix with meso- and macropores, which enhance bio-oil heavy component diffusion and attenuates the blockage of micropore entrance, because the meso- and macropores allow the placing and growth of the coke [52].

Table 2

Properties of the fresh catalyst and the deactivated catalysts, used in experiments with different bio-oil/methanol mass ratio.

Bio-oil/methanol Mass ratio (wt.%/wt.%)	Sample name	Sg ($\text{m}^2/\text{g}_{\text{cat}}$)	V_{mesopore} ($\text{cm}^3/\text{g}_{\text{cat}}$)	$V_{\text{micropore}}$ ($\text{cm}^3/\text{g}_{\text{cat}}$)	Acidity ($\text{mmol}_{\text{NH}_3}/\text{g}_{\text{cat}}$)
–	zNi (fresh)	177.7	0.57	0.034	0.41
40/60	α_{040} (alumina)	72.8	0.21	–	0.01
0/100	zNi ₀₀₀	125.3	0.53	0.016	0.13
40/60	zNi ₀₄₀	82.0	0.47	0.005	0.10
60/40	zNi ₀₆₀	78.6	0.45	0.002	0.08
100/0	zNi ₁₀₀	78.6	0.44	0.001	0.07

The physical properties of the fresh and deactivated catalysts (Table 2) have been determined by N_2 adsorption–desorption (Micromeritics ASAP 2010) and Hg porosimetry (Micromeritics Autopore 9220). Total acidity (Table 2) has been determined by measuring the differential adsorption of NH_3 at 150°C in a thermobalance (TA Instruments SDT 2960) on-line with a mass spectrometer (Balzers Instruments Thermostar) [53].

Table 2 also shows the properties of an α -alumina (supplied by Derivados del Fluor, Spain) with negligible acidity, which has been used as a catalyst to compare the results with those of the HZSM-5 zeolite acid catalyst.

2.3. Reaction and analysis equipment

The reaction equipment has been previously detailed [45] and consists of two reactors in-line (according to the Fig. 1). The first reactor (for the polymerization of lignin derivatives at 400°C) is a tube of S-316 stainless steel with an internal diameter of 159 mm, with a bed of glass spheres. The bio-oil inlet is cooled with water to avoid blockage. The output volatile stream enters the second reactor, which is a fluidized bed reactor (inside a vertical cylindrical tube made of S-316 stainless steel with an internal diameter of 20 mm and a total length of 465 mm) located within a ceramic chamber heated by an electrical resistance. The catalyst bed is placed on a porous plate (at 285 mm from the reactor base).

The experiments have been carried out under the following conditions: bio-oil/methanol mass ratio in the feed, between 100/0 and 0/100, 450°C , 1 atm and space time (based on the oxygenates in the bio-oil), $0.371 \text{ g}_{\text{catalyst}} \text{ h}(\text{g}_{\text{oxygenates}})^{-1}$. It is worth mentioning that space time is referred to the total content of oxygenates at the catalytic reactor inlet (those contained in the bio-oil remaining after pyrolytic lignin deposition and methanol co-fed). The deactivated catalyst samples are designated as zNi_x in the tables and figures, where x is the wt.% of bio-oil in the feed of bio-oil/methanol mixture.

The on-line analysis of the products is carried out every 5 min, with a gas chromatograph (Agilent Micro GC 3000) provided with

four modules for the analysis of the following: (1) permanent gases (O_2 , N_2 , H_2 , CO and CH_4); (2) oxygenates (MeOH, dimethyl ether and CO_2), light olefins (C_2 – C_3) and water; (3) C_2 – C_6 hydrocarbons; (4) C_6 – C_{12} hydrocarbons and oxygenate compounds.

2.4. Coke analysis

The TPO analysis of the coke deposited on the deactivated catalysts has been conducted by combustion with air in the TG/MS arrangement described above. Subsequent to a coke stripping step in a He stream at 550 °C for 1 h, combustion is carried out with 25% O_2 in He, following a ramp of 3 °C min^{-1} from 300 °C to 550 °C, and maintaining this temperature for 1 h. Stripping is necessary to remove the components of the reaction medium that are adsorbed on the catalyst. It has been proven that this stripping is not severe enough to partially reactivate the catalyst, so that the components removed cannot be considered constituents of the coke that deactivates the catalyst. However, if this stripping is not carried out, the adsorbed compounds interfere the results corresponding to the analysis of catalyst properties. Throughout combustion, the following data are monitored: temperature, mass, temperature difference between sample and reference and the intensity in the mass spectrometer for the signals corresponding to the masses 18 (water) and 44 (CO_2).

The FTIR spectra have been obtained in a Nicolet 6700 (Thermo), using a transmission cell, 60 scans, and a resolution of 4 cm^{-1} . The samples of deactivated catalysts (3–5 mg) have been pelletized with KBr (300 mg, purity >99%), applying pressures of 10 $t\ cm^{-2}$ for 10 min.

Raman spectra have been obtained in a Renishaw confocal microscope, using two lasers of 514 and 785 nm as excitation source, and subtracting the fluorescence caused by coke. The measurements have been carried out over 3–5 mg of deactivated catalyst, doing no less than 3 analyses in different positions and minimizing exposure to air to avoid coke oxidation.

The ^{13}C CP-MAS NMR (carbon-13 cross-polarization magic angle spinning nuclear magnetic resonance) experiments have been performed in a Broker DXR 300. Samples of deactivated catalysts (300 mg) have been placed in the container and analysed for 12–24 h.

In order to extract the soluble coke, 0.3–0.5 g of deactivated catalyst is exposed to 3–5 mL of HF (Merck, 40%) at 85 °C for 1 h. After drying and neutralization, coke extraction is performed in glass Soxhlet extractors using CH_2Cl_2 (Merck >99.8%), at 40 °C for 24 h. The extracts are analysed using simultaneously a gas chromatograph (Shimadzu GC-2010 with a TRB-1MS column) and a mass spectrometer (Shimadzu GCMS-QP2010).

3. Results

3.1. Catalyst deactivation by coke

Fig. 2 shows the evolution of bio-oil conversion with time on stream for different bio-oil/methanol mass ratios in the feed at 450 °C and a space time of $0.371\ g_{catalyst}\ h\ (g_{oxygenates})^{-1}$. The bio-oil conversion has been calculated from the mass flow rates of the oxygenated components in the bio-oil at the fluidized bed reactor inlet (remaining after the thermal polymerization step), $(m_{bio-oil})_{inlet}$, and outlet, $(m_{bio-oil})_{outlet}$:

$$X_{bio-oil} = \frac{(m_{bio-oil})_{inlet} - (m_{bio-oil})_{outlet}}{(m_{bio-oil})_{inlet}} \quad (1)$$

It is noted that after a rapid deactivation, the bio-oil conversion reaches a pseudo-stationary value after 3 h of time on stream. At zero time on stream and co-feeding methanol, bio-oil conversion

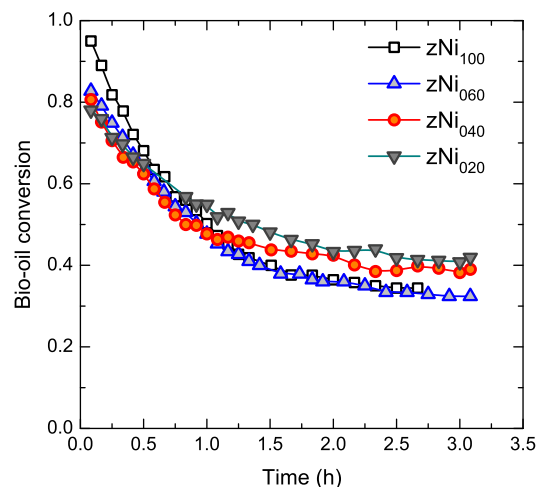


Fig. 2. Evolution with time on stream of bio-oil conversion for different bio-oil/methanol mass ratio in the feed at 450 °C and a space time of $0.371\ g_{catalyst}\ h\ (g_{oxygenates})^{-1}$.

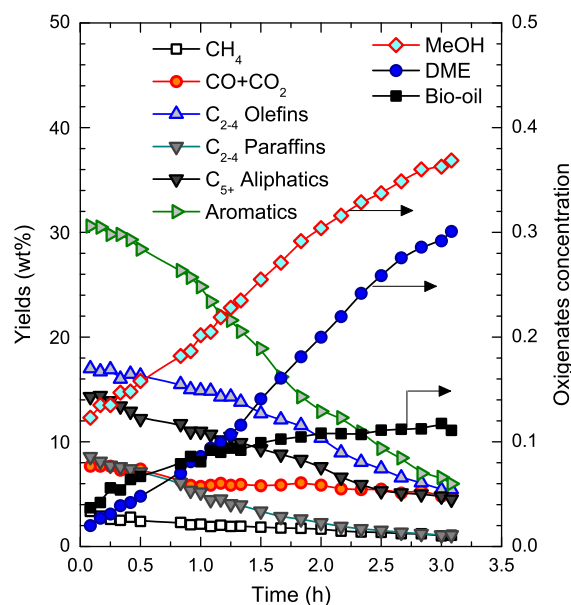


Fig. 3. Evolution of product yields (left axis) and oxygenate concentration (right axis) with time on stream for a feed of bio-oil/methanol with 20/80 mass ratio at 450 °C and a space time of $0.371\ g_{catalyst}\ h\ (g_{oxygenates})^{-1}$.

decreases due to the dilution of bio-oil oxygenated components. Nevertheless, the attenuating effect of deactivation is more significant, which has already been proven in a previous paper and is explained by the effect of methanol on the attenuation of bio-oil oxygenate polymerization [30].

Fig. 3 shows the evolution with time on stream of oxygenates (bio-oil, methanol and dimethyl ether) mass fraction at the reactor outlet, X_i , and reaction product yields, Y_i , on a water-free basis. These results correspond to a feed with a bio-oil/methanol mass ratio of 20/80, at 450 °C and a space time of $0.371\ g_{catalyst}\ h\ (g_{oxygenates})^{-1}$. Under these selected conditions, a high yield of aromatics is obtained [45]. The results in Fig. 3 are consistent with those obtained by Adjaye and Bakshi [54], who are pioneers in the study of catalytic transformation of bio-oil into hydrocarbons and showed the capacity of the HZSM-5 zeolite for obtaining selectively aromatics (toluene, xylenes and trimethyl benzene) and that

this zeolite has a greater deoxygenating capacity than other acid materials (H-mordenite and HY zeolites and silica-alumina) with lower yield of coke.

The yields in Fig. 3 have been calculated from the mass flow rates of each lump of products at the reactor outlet, $(m_i)_{\text{outlet}}$:

$$Y_i = \left[\frac{(m_i)_{\text{outlet}}}{(m_{\text{oxygenates}})_{\text{inlet}}} \right] \quad (2)$$

A comparison with the fresh catalyst shows that the physical properties and acidity of the deactivated catalysts (Table 2) have substantially been deteriorated due to deactivation. This deterioration is attenuated by decreasing the bio-oil/methanol ratio in the feed and is of lower significance for the catalyst used in the transformation of pure methanol. The deterioration in catalyst properties is related to the total amount of coke deposited, as discussed below. Furthermore, the decrease in acidity is less significant than in micropore volume, indicating that the catalyst maintains the acid sites accessible to the bio-oil, which are responsible for the remaining activity.

3.2. Thermal and catalytic coke

As an example of the TG-TPO results, Fig. 4 shows the TPO profile for the combustion of the carbonaceous material deposited on the catalyst for a feed of pure bio-oil (sample zNi₁₀₀). The extent of the TPO curve is characteristic of a heterogeneous coke made up of components with different H/C ratios [55]. Two fractions of coke are distinguished in the TPO curves corresponding to the feeds containing bio-oil. The fraction that burns at low temperature (peak in the 400–480 °C range) can be considered as a coke of thermal origin, formed by condensation–degradation of certain bio-oil oxygenated compounds (probably those derived from lignin pyrolysis because of their greater ability to polymerization), which are not completely separated in the thermal treatment step. This coke fraction is deposited on the meso- and macroporous structure of the catalyst matrix, and consequently, its combustion is less limited than the combustion of the catalytic coke, to which corresponds the second peak observed in the TPO curve. The other fraction of the coke is deposited on the HZSM-5 zeolite micropores and has been formed by evolution of the compounds in the reaction medium towards condensed and progressively less hydrogenated structures, by condensation reactions activated by the acid

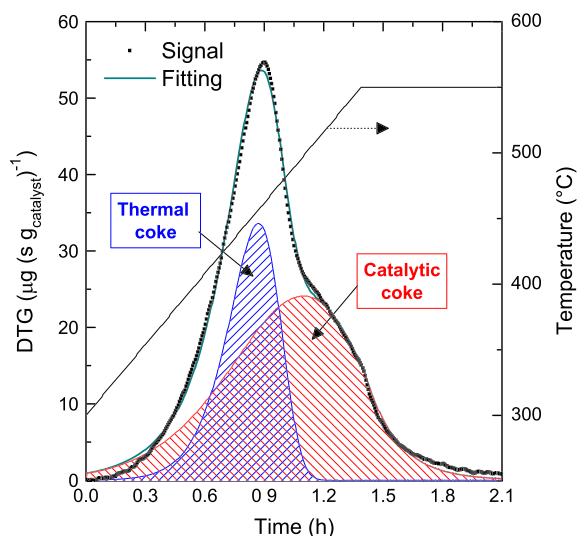


Fig. 4. TPO profile for the combustion of the coke deposited on the catalyst for a feed of pure bio-oil (sample zNi₁₀₀). Reaction conditions as in Fig. 2.

sites [56–58]. The hypothesis that the low temperature peak is a result of the coke combustion catalysed by Ni has been discarded, given that only the peak at high temperature is observed in the TPO analysis of the coke deposited in the experiments feeding pure methanol. In order to quantify both coke fractions, the TPO curve deconvolution has been calculated using a routine written in Matlab. This calculation considers the combustion of the two fractions of coke as two parallel kinetic events of first order, with respect to O₂ partial pressure (P_{O_2}) and to the content of each coke fraction (C_{ci}):

$$\frac{dC_{\text{ci}}}{dt} = k_i P_{\text{O}_2} C_{\text{ci}} = k_i^* \exp\left[\frac{-E_i}{R} \left(\frac{1}{T} - \frac{1}{T^*}\right)\right] P_{\text{O}_2} C_{\text{ci}} \quad (3)$$

The calculation solves the set of two differential equations (corresponding to Eq. (3) for both types of coke) and determines both coke fractions (Table 3) and the kinetic parameters for the combustion of each fraction.

By increasing the content of bio-oil in the feed, the total coke content and the content of thermal and catalytic coke fractions increase in the deactivated catalyst (Fig. 5). The fraction of thermal coke is insignificant for pure methanol in the feed, which confirms that thermal coke is due to the degradation of oxygenated components in the bio-oil. On the other hand, the attenuation of catalytic coke deposition by increasing the methanol content is consistent with the effect reported in the literature when the H/C ratio in the feed is increased in the oxygenate cracking [17,29,59].

The activation energy for thermal coke combustion is almost twice that corresponding to catalytic coke combustion ($E_{\text{thermal}} = 175 \pm 15 \text{ kJ mol}^{-1}$, $E_{\text{catalytic}} = 90 \pm 15 \text{ kJ mol}^{-1}$), whereas the kinetic constant at 550 °C is an order of magnitude higher than that for the catalytic coke ($k_{\text{thermal}}^* = 4.5 \pm 1.5 \times 10^{-2} \text{ atm}^{-1} \text{ s}^{-1}$, $k_{\text{catalytic}}^* = 3.5 \pm 0.5 \times 10^{-3} \text{ atm}^{-1} \text{ s}^{-1}$). This result is due to the aforementioned location of the thermal coke on the outside of the microporous structure of the zeolite, which makes its combustion easier. Consequently, thermal coke burns faster, and the peak in the TPO curve (Fig. 4) is narrower than that of catalytic coke. The oxygenated nature of this coke fraction enhances its combustion, as suggested by Moljord et al. [60,61], who found that coke combustion takes place through oxygenated intermediates generated by the oxidation of coke polyaromatics. In a previous paper, it was proven that the catalyst recovers completely its activity after coke combustion [46].

3.3. Properties of the coke

3.3.1. FTIR analysis

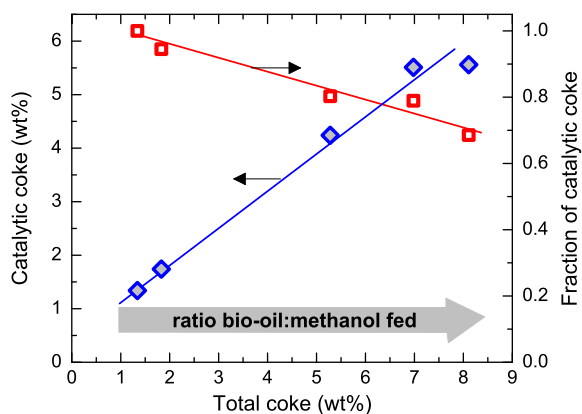
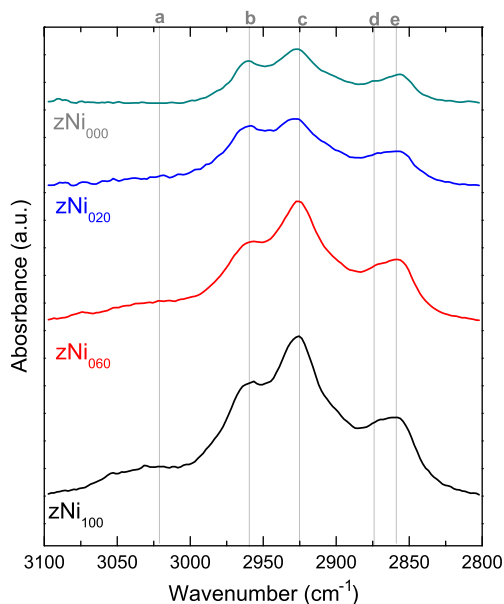
Fig. 6 shows the FTIR vibrational spectra of the coke deposited on the deactivated catalysts with feeds of different composition, in the spectral range of 2800–3100 cm^{-1} , corresponding to the vibrations of C–H bonds of paraffins and olefins (asymmetric and symmetric stretching) and single-ring aromatics [62]: (a) 3025 cm^{-1} , single-ring aromatics or alkyl aromatics; (b) 2960 cm^{-1} , –CH₃ groups; (c) 2900–2925 cm^{-1} , –CH₂ and –CH groups; (d) 2875 cm^{-1} , –CH₃ groups; (e) 2860 cm^{-1} , –CH₂ groups. The intensity of the bands corresponding to aliphatics and single-ring aromatics increases with increasing bio-oil/methanol mass ratio in the feed, and there is an increase in the number of terminal groups (–CH₃) as well as in length and/or cyclic groups (–CH and –CH₂) in the aliphatic chains. These results match those in literature for bio-oil cracking [63].

The intensities of the bands corresponding to conjugated double bonds, at 1500–1600 cm^{-1} , are similar for all samples, indicating that under these experimental conditions the intensity of the band at 1598 cm^{-1} is not related to the amount of coke (Table 3), as has been reported in the literature for other reactions [64,65]. This result is explained by the presence of alcoholic and carboxylic

Table 3

Coke contents of the deactivated catalysts, used in experiments with different bio-oil/methanol mass ratio, and results of the deconvolution of the TG-TPO profiles of coke.

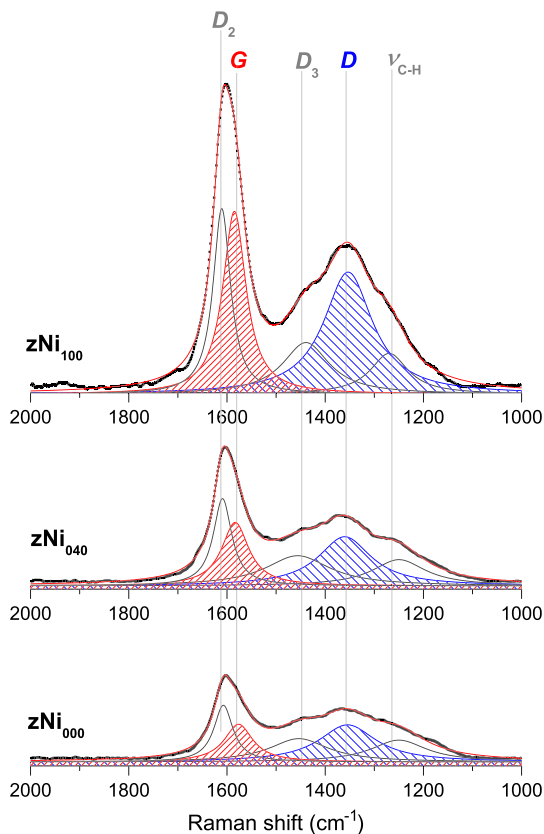
Bio-oil/methanol mass ratio (wt.%/wt.%)	Deactivated catalyst	(Cc) _{total} (wt.%)	(Cc) _{thermal} (wt.%)	(Cc) _{catalytic} (wt.%)
0/100	zNi ₀₀₀	1.34	0.00	1.34
20/80	zNi ₀₂₀	1.83	0.11	1.72
40/60	zNi ₀₄₀	5.28	1.04	4.24
60/40	zNi ₀₆₀	6.98	1.47	5.51
100/0	zNi ₁₀₀	8.11	2.55	5.56

**Fig. 5.** Evolution of catalytic coke content and its fraction in the total coke content for different bio-oil/methanol mass ratios in the feed. Reaction conditions as in Fig. 2.**Fig. 6.** FTIR spectra of the deactivated catalysts in the 2800–3100 cm⁻¹ region corresponding to aliphatic and aromatic vibrations: (a) single-ring aromatics or alkyl aromatics; (b) -CH₃ groups; (c) -CH₂ and -CH groups; (d) -CH₃ groups; (e) -CH₂ groups. Reaction conditions as in Fig. 2.

groups in the coke, which interfere with the vibrational bands of conjugated double bonds [63].

3.3.2. Raman spectroscopy

Fig. 7 shows the Raman spectra corresponding to the deactivated catalysts, using a 514-nm excitation laser. The spectra have been deconvoluted in 5 Lorentzian peaks [66]: (i) 1250–

**Fig. 7.** Raman spectra of the deactivated catalysts (with different bio-oil/methanol mass ratios in the feed) in the 1000–2000 cm⁻¹ region. Reaction conditions as in Fig. 2.

1270 cm⁻¹, C–H vibrations (ν_{C-H}); (ii) 1360 cm⁻¹, “breathing” vibrational mode of not-well-structured aromatics (*D* band); (iii) 1450 cm⁻¹, structural defects of aromatic clusters; (iv) 1575–1600 cm⁻¹, assigned to *in-plane* stretching vibrational modes of well-structured aromatics (*G* band); (v) 1610 cm⁻¹, also attributed to disordered aromatic structures.

Table 4 shows the intensities of the bands described above, the ratios of *D/G* band intensities (characteristic of the development of carbonaceous solids) and the values of coke particle size or *in-plane* correlation length (*L_a*) calculated using the Tuinstra–Koenig correlation [67]. The values of *G* band intensities increase with the content of bio-oil in the feed. This result indicates that the

Table 4

Intensities of the Raman bands corresponding to the spent catalysts.

Deactivated catalyst	ν_{C-H}	<i>D</i>	<i>D</i> ₃	<i>G</i>	<i>D</i> ₂	<i>D/G</i>	<i>L_a</i> (nm)
zNi ₀₀₀	0.29	0.36	0.09	0.13	0.13	2.80	1.57
zNi ₀₄₀	0.23	0.30	0.12	0.19	0.16	1.56	2.82
zNi ₁₀₀	0.09	0.34	0.14	0.24	0.19	1.41	3.12

proportion of the developed coke (band G) is related to the total amount of coke deposited on the catalyst (Table 3). Furthermore, the coke particle size (L_a) is higher as the total content of coke increases, so that the size of feeding pure methanol (zNi_{000}) is 1.57 nm and that of feeding bio-oil is double (3.12 nm for the sample zNi_{100}).

3.3.3. NMR spectroscopy

The profiles of ^{13}C CP-MAS NMR of deactivated catalysts are shown in Fig. 8. All catalysts show bands at 22 ppm and 129 ppm, corresponding to the carbonaceous nucleus of aliphatics, particularly $-CH_3$ groups and aromatics, respectively [63]. In feeding pure methanol (zNi_{000}), the only bands observed are those associated with aromatics and aliphatics, with the aliphatics/aromatics ratio higher than those for the catalysts deactivated with bio-oil containing feeds. This result confirms that the coke formed in the conversion of methanol is made up of aromatic species multi-substituted with $-CH_3$ groups, which is consistent with the secondary mechanism for coke formation known as “hydrocarbon pool” mechanism for methanol transformation into hydrocarbons [68,69]. The catalysts that have been deactivated with a bio-oil containing feed present a low-intense band at 181 ppm, which is assignable to carboxylic acid groups in the coke. By increasing the bio-oil/methanol ratio in the feed, the band of carboxylic groups is more notable, whereas the band of aromatics becomes more intense than that of aliphatics. Moreover, the catalysts deactivated with a feed of pure bio-oil (zNi_{100}) present an aromatic band with a shoulder at 150 ppm, evidencing its nature of aromatic coke, which is more condensed and crystalline [63] than for the other samples corresponding to feeds with lower content of bio-oil. In addition, increasing the bio-oil/methanol mass ratio in the feed, the aliphatic band becomes wider due to the existence of more aliphatic carbon nucleus. Fig. 9 shows that the ratio between the intensities of the bands corresponding to aromatic and aliphatic components of coke increases linearly with the content of catalytic coke fraction.

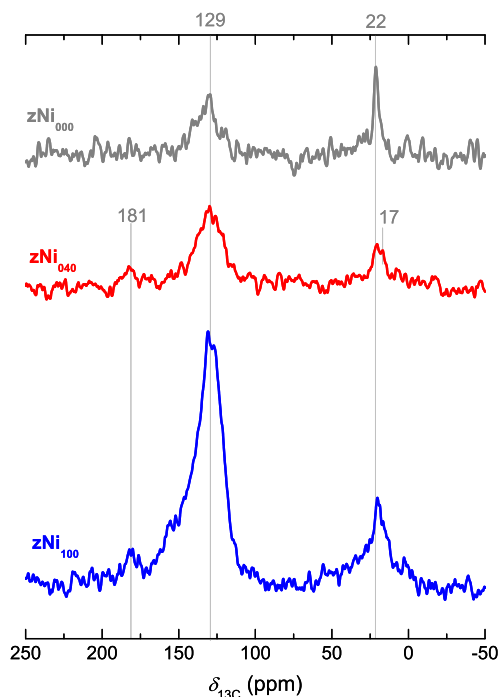


Fig. 8. ^{13}C NMR spectra of the deactivated catalysts (with different bio-oil/methanol mass ratios in the feed). Reaction conditions as in Fig. 2.

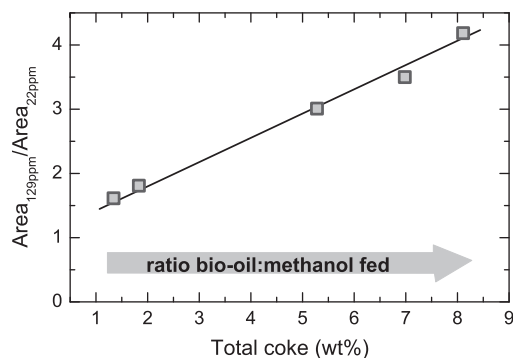


Fig. 9. Ratio of aromatics (129 ppm)/aliphatics (22 ppm) area versus the coke content of the deactivated catalysts (with different bio-oil/methanol mass ratios in the feed) based on the results of ^{13}C NMR. Reaction conditions as in Fig. 2.

3.3.4. Extraction and analysis of soluble coke

Fig. 10 shows the content of CH_2Cl_2 insoluble coke (quantified by TG-TPO) and the contents of different component families in CH_2Cl_2 soluble coke, determined by GC/MS analysis, for the catalyst deactivated with the different feeds. Furthermore, the composition is shown for a coke (of thermal origin) deposited on non-catalytic material ($\alpha-Al_2O_3$, named a_{040} , tested under the same conditions as the HZSM-5 catalyst deactivated with a bio-oil/methanol mass ratio in the feed of 40/60). The difference between the amount and composition of the coke deposited on the $\alpha-Al_2O_3$ and on the HZSM-5 catalyst is notable and highlights the importance of catalyst acidity for the formation of thermal and catalytic coke fractions. A low coke content is deposited on the $\alpha-Al_2O_3$ (only of thermal origin) due to the insignificant activity of this material for the transformation of methanol and bio-oil into hydrocarbons. This thermal coke is composed mainly of oxygenates and oxo-aromatics, with a small proportion of aliphatics, proving that aromatics and aliphatics are mainly formed by the catalytic pathway of deactivation. The sample of HZSM-5 catalyst deactivated under the same conditions (zNi_{40}) has a higher content of both fractions of coke, and in addition to oxygenated and aromatic compounds, it has a significant content of aliphatics and aromatics and a higher content of soluble coke. A comparison of the results shows that the acid sites of the catalyst activate

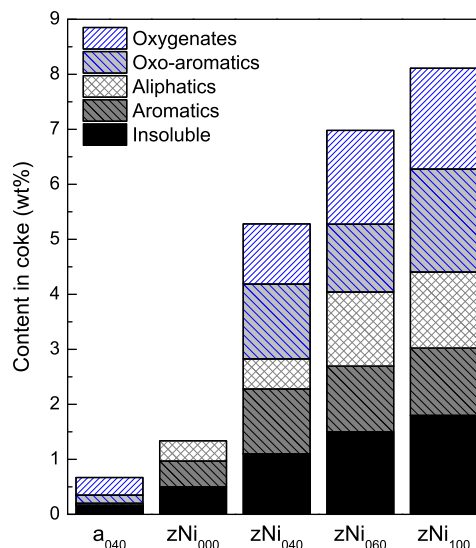


Fig. 10. Composition of the coke deposited on the deactivated catalysts (with different bio-oil/methanol mass ratios in the feed) and on the inert material (α -alumina). Reaction conditions as in Fig. 2.

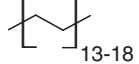
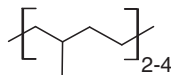
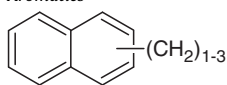
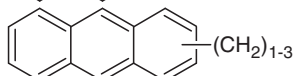
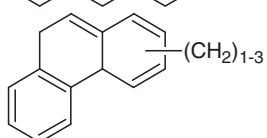
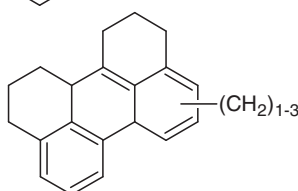
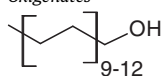
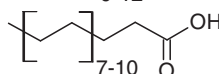
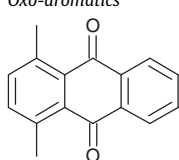
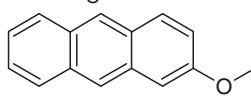
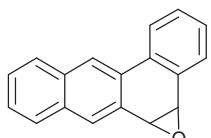
both the steps for the formation of the so-called catalytic coke and the deposition of the so-called thermal coke, which is attributed to the polymerization of the products derived from the pyrolysis of biomass lignin.

As observed in Fig. 10, the amount of insoluble coke increases with the content of bio-oil in the feed, although the ratio of soluble to insoluble within the coke does not vary significantly. This result is explained by considering the evolution of the different fractions of coke to more dehydrogenated structures. The results soluble coke composition evidence that, as the bio-oil/methanol ratio in the feed is increased, the amount of all coke fractions increases (as does the total coke content), especially that of oxygenate and oxo-aromatic compounds. These oxygenated fractions are not

present in the coke obtained with a feed of pure methanol, which means a non-oxygenated nature with aliphatic and aromatic hydrocarbons as major components.

The components representative of each family of the soluble coke fraction are shown in Table 5. The aliphatic lump is mainly composed of hydrocarbon structures, with low branching and low number of insaturations, with approximately 15–20 carbons. The aromatic lump is made up of structures of 2 and 3 rings and, to a lesser extent, of up to 5 (benzopyrene). The oxygenates have components with alcoholic- or carboxylic groups and with lower number of carbons than aliphatics. Table 5 shows the structure of three oxo-aromatics that are representative of those contained in the coke.

Table 5
Main components of each family of the soluble coke, extracted from the spent catalysts.

<i>Aliphatics</i>	
	Aliphatics C ₁₅ –C ₂₀
	Branched aliphatics C ₁₁ –C ₁₈
<i>Aromatics</i>	
	Naphthalene (methyl, dimethyl and trimethyl)
	Anthracene (methyl, dimethyl and trimethyl)
	Phenanthrene (methyl, dimethyl and trimethyl)
	Hexahydroperylene
<i>Oxygenates</i>	
	Alcohols C ₁₁ –C ₁₄
	Acids C ₁₁ –C ₁₄
<i>Oxo-aromatics</i>	
	1,4-Dimethyl-9,10-anthracenedione,
	2-Methoxy-6-methylantracene
	1a, 11b-Dihydro-1-methylbenz[3,4]anthra[1,2b]oxigene

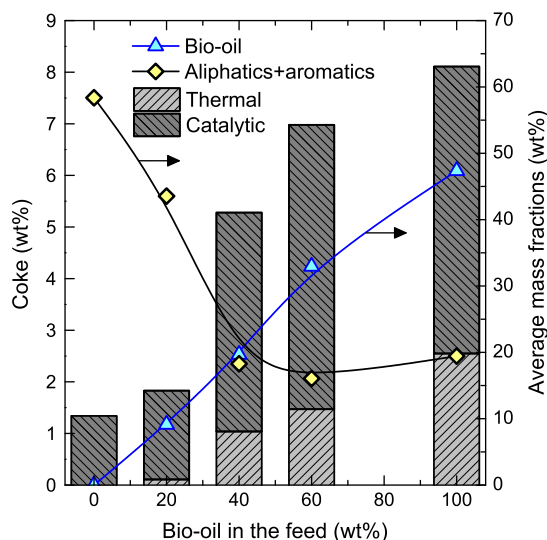


Fig. 11. Evolution with bio-oil content in the feed of coke contents (total, thermal and catalytic) and average mass fractions in the reaction medium of bio-oil and hydrocarbons. Reaction conditions as in Fig. 2.

3.4. Effect of reaction medium on deactivation

In this study, the conditions of the experiments correspond to a low value of space–time, for which the catalyst undergoes rapid deactivation by coke deposition. Under these conditions of rapid deactivation, the reaction medium is a crucial factor. The importance of reaction medium concentration on coke formation is essential for the transformation into hydrocarbons of pure oxygenates, such as methanol [25–27] and ethanol [52,70–72], in which the role of oxygenated reactant concentration in the formation of catalytic coke over HZSM-5 zeolite catalysts has been extensively reported. In the transformation of bio-oil into hydrocarbons, Gayubo et al. [44] and Valle et al. [45] have proven that increasing space–time and, therefore, the catalyst/bio-oil flow rate and bio-oil conversion (decreasing the bio-oil concentration in the medium), the total coke content and the thermal and catalytic coke fractions decrease significantly. This result should be considered when assessing the viability of the process, because space–time is a condition that must be optimized in large-scale processes.

Furthermore, it should be noted that the coke analysed corresponds to a catalyst deactivated for 3 h of time on stream, for which the cracking ability of the catalyst decreases in addition to the steady decrease in the hydrocarbon concentration in the reaction medium and increase in the bio-oil oxygenate concentration.

The different composition of the reaction medium is taken into account in Fig. 11, which shows the relationship between coke contents (total, thermal and catalytic) and the average mass fractions of hydrocarbons and bio-oil in the reaction medium for 3 h. It is noted that the decrease in hydrocarbon yield and the increase in bio-oil mass fraction (unreacted) occur simultaneously with an increase in total coke content and thermal and catalytic coke on the catalyst. These results are consistent with the effect expected for the oxygenate concentration in the medium, i.e. enhancing the formation of both coke fractions.

4. Discussion

A simplified kinetic scheme proposed for the transformation of bio-oil/methanol mixture into hydrocarbons and coke over HZSM-5-based catalysts is shown in Fig. 12. This scheme has differences with those reported for the conversion of methanol into hydrocar-

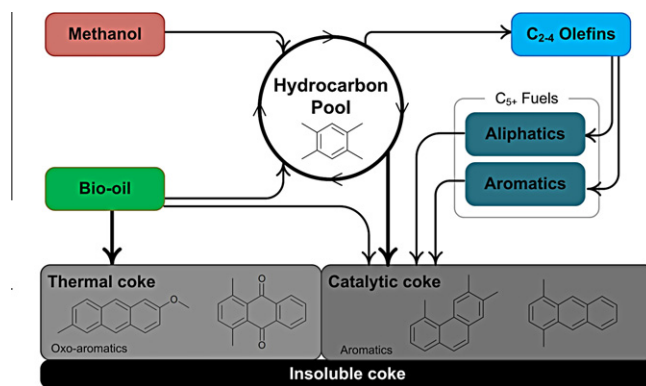


Fig. 12. Kinetic scheme proposed for the transformation of bio-oil/methanol mixture into hydrocarbons and coke over HZSM-5-based catalysts. Reaction conditions as in Fig. 2.

bons over HZSM-5 zeolite. Firstly, a coke fraction is formed by polymerization of certain bio-oil oxygenates derived from the pyrolysis of biomass components (lignin, cellulose and hemicellulose). This polymerization is presumably favoured by the acid sites of the catalyst and attenuated by the methanol content in the feed [30].

The results of deterioration of catalyst properties (Table 2) show that much of the microporous and acid structure of the catalyst is blocked by the coke. However, assuming the worst scenario of pure graphitic coke (with a density of 2.23 g cm^{-3}) plugging all the micropores, the deactivated catalyst would eventually have a coke content of 7.5 wt%. Combining these data with those of coke composition (Fig. 10 and Table 3, which indicate that the coke density must be substantially lower than that of graphite), it can be concluded that a significant fraction of the coke is deposited outside the zeolite crystals, which is consistent with the TPO results.

Furthermore, the structure of the catalytic coke in the transformation of bio-oil/methanol mixtures (mostly located inside HZSM-5 zeolite crystals) is different to the specific coke deposited in the transformation of pure methanol. Methanol conversion goes through the “hydrocarbon pool” mechanism with methyl benzenes as intermediates for the formation of light olefins as primary products [68,69]. These intermediates become inert when the benzene ring is saturated with methyl groups, and these polymethyl benzenes (with five or six methyl groups) are the precursors of subsequent condensations towards polyaromatic structures that are retained in the crystal channels of the zeolite [73,74]. This interpretation, based on spectroscopic observations proving the existence of benzene intermediates, is supported by kinetic studies of deactivation, which have highlighted the dependence of the deactivation kinetics with methanol concentration in the feed [25,75]. This mechanism for coke formation from methanol occurs simultaneously to the extensively reported steps for coke formation from the reaction hydrocarbon products, through oligomerization–cyclization–aromatization–condensation reactions catalysed by the acid sites of the catalyst [56–58,74]. It is noteworthy that the reaction conditions used in this paper (high temperature, 450°C , and a suitable catalyst for the formation of aromatics and with dehydrogenating activity due to the presence of Ni) favour the formation of coke from the hydrocarbons in the reaction medium.

The aforementioned results show that co-feeding bio-oil significantly contributes to the formation of catalytic coke, apart from being responsible for the deposition of thermal origin coke. The analysis of coke gives way to a better comprehension of the species forming the thermal and catalytic coke. By correlating the thermal and catalytic coke results (Table 3) with those of coke composition

(Fig. 10), it can be concluded that the oxygenates in the soluble coke are the constituents of the thermal coke. The analysis of this coke allows establishing that it is a heterogeneous coke, with alcoholic and carboxylic groups and with the presence of oxo-aromatics. Furthermore, the content of the catalytic coke deposited increases with the bio-oil/methanol mass ratio in the feed, which also gives way to an increase in the aromatic character of the coke and its condensation and evolution towards a graphitic structure.

Based on these results, the catalytic coke can be considered a material evolving towards a polycondensed structure insoluble in CH_2Cl_2 , which is generated by several routes activated by the acid sites: (i) from methanol by the “hydrocarbon pool” mechanism, which generates polyaromatic structures that are retained in the HZSM-5 zeolite crystals; (ii) by condensation of the hydrocarbon products in the cracking-deoxygenation reactions of bio-oil components; (iii) by condensation of the intermediates in the mentioned reactions; and (iv) by condensation of the coke components originally deposited as a result of the polymerization of products derived from the pyrolysis of biomass lignin.

There is probably a synergy between the routes for catalytic coke formation from methanol and from bio-oil due to the contribution of bio-oil derivatives in the hydrocarbon pool mechanism. This hypothesis is consistent with the results by Carlson et al. [14,15], who established a mechanism based on the oxygenated intermediates in the reaction and hydrocarbons produced (especially olefins and aromatics) for coke formation in the cracking of glucose. Chen and Huber [28] studied the formation of coke from a pure compound (furan as a model of cellulosic biomass) and confirm the possible existence of a hydrocarbon pool from which the coke derives as a by-product. Given the complexity of the bio-oil, a better understanding of this synergy would require the study of the coke deposited in the reactions by co-feeding different bio-oil components with methanol.

5. Conclusions

The co-feeding of crude bio-oil with methanol is interesting for its large-scale valorization, because it can be carried out under reaction conditions similar to those reported for methanol conversion into hydrocarbons, based on the technological development of the fluidized bed reactor and the HZSM-5 zeolite catalyst, which have been widely studied for selectively obtaining fuel in the range of gasoline, light olefins or BTX aromatics. The availability of a previous step in-line allows a controlled separation of most of the bio-oil oxygenates derived from the pyrolysis of lignocellulosic biomass lignin, which repolymerize in this step at 400 °C and form a carbonaceous material (called pyrolytic lignin) with lignin-like structure.

The catalyst deactivation in the catalytic step is due to coke deposition, which according to its origin has two fractions. The fraction of thermal origin (characteristic of bio-oil co-feeding) is presumably formed by the polymerization (favoured by the acid sites) of certain oxygenated compounds that have not been polymerized in the first step and are deposited in the meso- and macropores structure of the catalyst matrix. The coke of catalytic origin is formed by condensation of intermediates of the cracking-deoxygenation reactions that undergo the oxygenated bio-oil components and by well-established mechanisms in the literature for coke formation from the hydrocarbons produced. The coke formed from the intermediates of the “hydrocarbon pool” mechanism for methanol transformation into hydrocarbons and the coke formed from the hydrocarbons in the reaction medium also contribute to this fraction. This catalytic coke is deposited mainly within the crystal channels of HZSM-5 zeolite, although it is also partially deposited outside the crystals, for which the matrix is effective.

Another feature of the coke deposited when bio-oil is co-fed with methanol is its heterogeneous and oxygenated nature, with the presence of oxo-aromatics, alcoholic and carboxylic groups, which are associated with the evolution of thermal origin coke that is deposited mainly outside the zeolite crystals. The catalytic coke produced when feeding pure methanol is not oxygenated and has a high content of polymethyl aromatics.

There is evidence that an increase in the bio-oil/methanol mass ratio in the feed has a remarkable effect on the coke content, its origin and nature. By increasing this ratio, the total coke content and the thermal and catalytic fraction contents increase. It is noteworthy that the catalytic coke is more aromatic and its condensation degree is higher, which allows establishing a possible synergy between the mechanisms for coke formation from methanol and bio-oil. However, given the complexity of bio-oil composition, it would be interesting to know the nature of the catalytic coke formed in the transformation of key compounds.

Acknowledgments

This work was carried out with the financial support of the Department of Education Universities and Investigation of the Basque Government (Project GIC07/24-IT-220-07) and of the Ministry of Science and Innovation of the Spanish Government (Projects CTQ2006-12006/PPQ and CTQ2010-19623/PPQ).

References

- [1] G.W. Huber, S. Iborra, A. Corma, *Chem. Rev.* 106 (2006) 4044–4098.
- [2] A. Demirbas, *Appl. Energy* 88 (2011) 17–28.
- [3] P.S. Nigam, A. Singh, *Prog. Energy Combust. Sci.* 37 (2011) 52–68.
- [4] R. Aguado, M. Olazar, M.J. San José, G. Aguirre, J. Bilbao, *Ind. Eng. Chem. Res.* 39 (2000) 1925–1933.
- [5] S. Kim, S. Jung, J. Kim, *Bioresour. Technol.* 101 (2010) 9294–9300.
- [6] S. Czernick, A. Bridgwater, *Energy Fuels* 18 (2004) 590–598.
- [7] M. García-Perez, A. Chaala, H. Pakdel, D. Kretschmer, C. Roy, *Biomass Bioenergy* 31 (2007) 222–242.
- [8] D. Mohan, C.U. Pittman, P.H. Steele, *Energy Fuels* 20 (2006) 848–889.
- [9] M. Stöcker, *Angew. Chem. Int. Ed.* 48 (2008) 9200–9211.
- [10] M. Olazar, R. Aguado, A. Barona, J. Bilbao, *AIChE J.* 46 (2000) 1025–1033.
- [11] A. Atutxa, R. Aguado, A.G. Gayubo, M. Olazar, J. Bilbao, *Energy Fuels* 19 (2005) 765–774.
- [12] A. Aho, N. Kumar, K. Eränen, T. Salmi, M. Hupa, D.Y. Murzin, *Trans. IChemE. E. B* 85 (2007) 473–480.
- [13] A. Aho, N. Kumar, K. Eränen, T. Salmi, M. Hupa, D.Y. Murzin, *Fuel* 87 (2008) 2493–2501.
- [14] T.R. Carlson, T.R. Vispute, G.W. Huber, *ChemSusChem* 1 (2008) 397–400.
- [15] T.R. Carlson, J. Jae, Y.C. Lin, G.A. Tompsett, G.W. Huber, *J. Catal.* 270 (2010) 110–124.
- [16] A. Aho, N. Kumar, A.V. Lahlul, K. Eränen, M. Ziolek, P. Decyk, T. Salmi, B. Holmbom, M. Hupa, D.Y. Murzin, *Fuel* 89 (2010) 1992–2000.
- [17] R. French, S. Czernik, *Fuel Process. Technol.* 91 (2010) 25–32.
- [18] A. Pattiya, J.O. Titiloye, A. Bridgwater, *Fuel* 89 (2010) 244–253.
- [19] A. Corma, H. Huber, L. Sauvinaud, P. ÓConnor, *J. Catal.* 247 (2007) 307–327.
- [20] X. Dupain, D.J. Costa, C.J. Schaverien, M. Makkee, J.A. Moulijn, *J. Appl. Catal. B* 72 (2007) 44–61.
- [21] I. Graça, F. Ramôa Ribeiro, H.S. Cerqueira, Y.L. Lam, M.B.B. de Almeida, *Appl. Catal. B* 90 (2009) 556–563.
- [22] I. Graça, J.M. Lopes, M.F. Ribeiro, F. Ramôa Ribeiro, H.S. Cerqueira, M.B.B. de Almeida, *Appl. Catal. B* 101 (2011) 613–621.
- [23] A.G. Gayubo, A.T. Aguayo, A. Atutxa, R. Aguado, J. Bilbao, *Ind. Eng. Chem. Res.* 43 (2004) 2610–2618.
- [24] A.G. Gayubo, A.T. Aguayo, A. Atutxa, R. Aguado, M. Olazar, J. Bilbao, *Ind. Eng. Chem. Res.* 43 (2004) 2619–2626.
- [25] A.G. Gayubo, A.T. Aguayo, M. Castilla, M. Olazar, J. Bilbao, *AIChE J.* 48 (2002) 1561–1575.
- [26] A.G. Gayubo, A.T. Aguayo, M. Olazar, R. Vivanco, J. Bilbao, *Chem. Eng. Sci.* 58 (2003) 5239–5249.
- [27] A.T. Aguayo, D. Mier, A.G. Gayubo, M. Gamero, J. Bilbao, *Ind. Eng. Chem. Res.* 49 (2010) 12371–12378.
- [28] Y.T. Chen, G.W. Huber, *ACS Catal.* 1 (2011) 611–628.
- [29] U.V. Mentzel, M.S. Holm, *Appl. Catal. A* 396 (2011) 59–67.
- [30] A.G. Gayubo, B. Valle, A.T. Aguayo, M. Olazar, J. Bilbao, *Energy Fuels* 23 (2009) 4129–4136.
- [31] A.G. Gayubo, A.T. Aguayo, A. Atutxa, B. Valle, J. Bilbao, *J. Chem. Technol. Biotechnol.* 80 (2005) 1244–1251.

- [32] A.G. Gayubo, A.T. Aguayo, A. Atutxa, R. Prieto, J. Bilbao, *Energy Fuels* 18 (2004) 1640–1647.
- [33] W. Li, Ch. Pan, Q. Zhang, Z. Liu, J. Peng, P. Chen, H. Lou, X. Zheng, *Bioresour. Technol.* 102 (2011) 4884–4889.
- [34] A. Oasmaa, E. Kuoppala, S. Gust, Y. Solantausta, *Energy Fuels* 17 (2003) 1–12.
- [35] M. Bertero, G. de la Puente, U. Sedran, *Energy Fuels* 25 (2011) 1267–1275.
- [36] F. de Miguel Mercader, M.J. Groeneveld, S.R.A. Kersten, N.W.J. Way, *Appl. Catal. B* 96 (2010) 57–66.
- [37] G. Fogassy, N. Thegarid, G. Toussaint, A.C. van Veen, Y. Schuurman, C. Mirodatos, *Appl. Catal. B* 96 (2010) 476–485.
- [38] J. Wildschut, I. Melian-Cabrera, H. Heeres, *Appl. Catal. B* 99 (2010) 298–306.
- [39] J. Diebold, S. Czernik, *Energy Fuels* 11 (1997) 1081–1091.
- [40] R. Hilten, K. Das, *Fuel* 89 (2010) 2741–2749.
- [41] R. Hilten, B. Bibens, J. Kastner, K. Das, *Energy Fuels* 24 (2010) 673–682.
- [42] L. Moens, S. Black, M. Myers, S. Czernik, *Energy Fuels* 23 (2009) 2695–2699.
- [43] A.G. Gayubo, B. Valle, A.T. Aguayo, M. Olazar, J. Bilbao, *J. Chem. Technol. Biotechnol.* 85 (2010) 132–144.
- [44] A.G. Gayubo, B. Valle, A.T. Aguayo, M. Olazar, J. Bilbao, *Ind. Eng. Chem. Res.* 49 (2010) 123–131.
- [45] B. Valle, A.G. Gayubo, A.T. Aguayo, M. Olazar, J. Bilbao, *Energy Fuels* 24 (2010) 2060–2070.
- [46] B. Valle, A.G. Gayubo, A. Alonso, A.T. Aguayo, J. Bilbao, *Appl. Catal. B* 100 (2010) 318–327.
- [47] J. Palomar, J. Lemus, M.A. Gilarranz, J.J. Rodríguez, *Carbon* 47 (2009) 1846–1856.
- [48] Z.M. de Pedro, J.A. Casas, L.M. Gómez-Sainero, J.J. Rodríguez, *Appl. Catal. B* 98 (2010) 79–85.
- [49] J. Bedia, R. Barrionuevo, J. Rodríguez-Mirasol, T. Cordero, *Appl. Catal. B* 103 (2011) 302–310.
- [50] B. Valle, A. Alonso, A. Atutxa, A.G. Gayubo, J. Bilbao, *Catal. Today* 106 (2005) 118–122.
- [51] P.L. Benito, A.T. Aguayo, A.G. Gayubo, J. Bilbao, *Ind. Eng. Chem. Res.* 35 (1996) 2177–2182.
- [52] A.G. Gayubo, A. Alonso, B. Valle, A.T. Aguayo, J. Bilbao, *Appl. Catal. B* 97 (2010) 299–306.
- [53] A.T. Aguayo, A.G. Gayubo, R. Vivanco, M. Olazar, J. Bilbao, *Appl. Catal. A* 283 (2005) 197–207.
- [54] J.D. Adjaye, N.N. Bakhsi, *Fuel Process. Technol.* 45 (1995) 161–183.
- [55] J.M. Ortega, A.G. Gayubo, A.T. Aguayo, P.L. Benito, J. Bilbao, *Ind. Eng. Chem. Res.* 36 (1997) 60–66.
- [56] M. Guisnet, P. Magnoux, *Appl. Catal. A* 212 (2001) 83–96.
- [57] M. Guisnet, L. Costa, F. Ramôa Ribeiro, *J. Mol. Catal. A* 305 (2009) 69–83.
- [58] H.S. Cerqueira, G. Caeiro, L. Costa, F. Ramôa Ribeiro, *J. Mol. Catal. A* 292 (2008) 1–13.
- [59] N.Y. Chen, T.F. Degan Jr., L.R. Koenig, *Chemtech* 16 (1986) 506–511.
- [60] K. Moljord, P. Magnoux, M. Guisnet, *Catal. Lett.* 25 (1994) 141–147.
- [61] K. Moljord, P. Magnoux, M. Guisnet, *Catal. Lett.* 28 (1994) 53–59.
- [62] P. Castaño, G. Elordi, M. Olazar, A.T. Aguayo, B. Pawelec, J. Bilbao, *Appl. Catal. B* 104 (2011) 91–100.
- [63] X. Guo, Y. Zheng, B. Zhang, J. Chen, *Biomass Bioenergy* 33 (2009) 1469–1473.
- [64] H.G. Karge, W. Niessen, H. Bludau, *Appl. Catal. A* 146 (1996) 339–349.
- [65] H.G. Karge, J. Weitkamp (Eds.), *Molecular Sieves. Characterization II*, vol. 5, Springer, Berlin, 1999.
- [66] B. Guichard, M. Roy-Auberger, E. Devers, B. Rebours, A.A. Quoineaud, M. Digne, *Appl. Catal. A* 367 (2009) 1–8.
- [67] F. Tuinstra, J.L. Koenig, *J. Chem. Phys.* 53 (1970) 1126.
- [68] A.T. Aguayo, A.G. Gayubo, R. Vivanco, A. Alonso, J. Bilbao, *Ind. Eng. Chem. Res.* 44 (2005) 7279–7286.
- [69] M. Bjorgen, S. Svelle, F. Joensen, J. Nerlov, S. Kolboe, F. Bonino, L. Palumbo, S. Bordiga, U. Olsbye, *J. Catal.* 249 (2007) 195–207.
- [70] A.G. Gayubo, A. Alonso, B. Valle, A.T. Aguayo, J. Bilbao, *Ind. Eng. Chem. Res.* 49 (2010) 10836–10844.
- [71] A.G. Gayubo, A. Alonso, B. Valle, A.T. Aguayo, M. Olazar, J. Bilbao, *Fuel* 89 (2010) 3365–3372.
- [72] A.G. Gayubo, A. Alonso, B. Valle, A.T. Aguayo, M. Olazar, J. Bilbao, *Chem. Eng. J.* 167 (2011) 262–277.
- [73] Y. Jiang, J. Huang, V.R. Reddy Marthala, Y.S. Ooi, J. Weitkamp, M. Hunger, *Micropor. Mesopor. Mater.* 105 (2007) 132–139.
- [74] H. Schulz, *Catal. Today* 154 (2010) 183–194.
- [75] P.L. Benito, A.G. Gayubo, A.T. Aguayo, M. Castilla, J. Bilbao, *Ind. Eng. Chem. Res.* 35 (1996) 81–89.